IN SITU NEUTRON TRANSMISSION BRAGG EDGE MEASUREMENTS OF STRAIN FIELDS NEAR FATIGUE CRACKS GROWN IN AIR AND IN HYDROGEN

MATTHEW CONNOLLY
National Institute of Standards and Technology
Boulder, CO, USA

PETER BRADLEY
National Institute of Standards and Technology
Boulder, CO, USA

ANDREW SLIFKA
National Institute of Standards and Technology
Boulder, CO, USA

ELIZABETH DREXLER
National Institute of Standards and Technology
Boulder, CO, USA

ABSTRACT

In situ transmission Bragg edge measurements of the strain fields in an X70 steel were performed near fatigue cracks grown in air and in hydrogen. Through the use of a novel test chamber which is capable of pressurization with hydrogen gas, and amenable to neutron-scattering measurements, fatigue cracks were grown in X70 steel specimens at the NG-6 neutron-imaging beam line at the NIST Center for Neutron Research. The measured strain fields are presented and discussed in the context of proposed mechanisms of hydrogen-assisted fatigue crack growth.

INTRODUCTION

Pipelines are the most likely means of transporting gaseous hydrogen to support clean power generation and clean transportation[1]. Although steels are a cost-effective solution for the construction of hydrogen gas pipelines, their fatigue and fracture properties are adversely affected by the presence of gaseous hydrogen[2-4]. The corrosive effect of hydrogen on steels manifests in fatigue crack growth rates (FCGRs) which are one to two orders of magnitude faster when grown in H_2 compared with those grown in air. Although the embrittlement effect has been observed since 1875[5], the exact mechanism (or mechanisms) that dominates remains to be elucidated. Until recently, most hydrogen embrittlement research comprised anecdotal material-specific observations, and concentrated on urgent technical problems[6]. Determination of the mechanism(s) is necessary to develop designs for high-functioning hydrogen transportation and storage applications, which may, in turn, provide insight into hydrogen effects in other material classes.

The National Institute of Standards and Technology (NIST) has an ongoing program to generate hydrogen-assisted FCGR (HA-FCGR) data[7]. The laboratory at NIST is one of only a few capable of performing FCGR measurements in gaseous hydrogen — the same failure mode that would be expected in service. The program has recently begun expanding to complement

in-air and HA-FCGR data with physics-based modeling and a scientific corroboration of the prevailing mechanisms. Ultimately, the goal is to use the data collected at NIST to create and calibrate a physics-based predictive model for the damage and deformation response of pipeline steels in gaseous hydrogen.

There exist several proposed mechanisms of embrittlement including hydrogen-enhanced decohesion (HEDE) and hydrogen-enhanced localized plasticity (HELP)[8-9]. In the HEDE mechanism, interstitial accumulation of hydrogen at locations of high triaxial stresses leads to the weakening of Fe-Fe bonds once the hydrogen concentration reaches a critical concentration. In the HELP mechanism, the introduction of hydrogen gas creates areas of extended dislocations in the Fe lattice and enhances dislocation mobility in the steel framework. A full quantification of the elastic and plastic deformation as a function of stress and hydrogen concentration is not yet determined.

Neutron-diffraction measurements of strain in steel are readily available to study elastic lattice deformation leading to HA-FCGR. In these measurements, a spatial mapping of the atomic lattice spacing is produced. With an appropriate measurement of an unstressed lattice spacing, the measured lattice spacing during mechanical loading can then determine the elastic lattice strain. However, the determination of strain fields near fatigue cracks grown in H_2 is challenging experimentally, because of the rapid diffusion of hydrogen from the steels. Even after extended exposure to H_2, in-air FCGRs are observed in steels once the specimen is removed from the H_2 [10]. In order to fully understand the HA-FCGR mechanism, it is necessary to perform any measurements in situ. To achieve this, a test chamber has been developed that can hold moderate gas pressure (3.4 MPa, 500 psi), and has the capability of mechanical loading of steel specimens for neutron and synchrotron x-ray scattering measurements. The chamber has been designed to be nearly transparent to neutron radiation, ideal for diffraction and radiography. The chamber is compatible with load frames available at the user facilities at Argonne National Laboratory Advanced Photon Source, the NIST Center for Neutron Research, and Oak Ridge National Laboratory Spallation Neutron Source.

In this paper, we present neutron Transmission Bragg Edge Spectroscopy (TBES) measurements of the strain fields around crack tips grown via fatigue in air and in a hydrogen environment. Drastic differences in both magnitude and spatial extent of the crack tip strain fields grown in each condition are demonstrated.

MATERIALS

The material used for this study was an X70 pipeline steel. The material was chosen due to its heavy use in pipelines as well as the abundance of in-air and hydrogen-assisted FCGR data on the material. Table 1 shows the chemical composition of the material used in this study; the balance is Fe. Table 2 shows the tensile properties of the material used in this study. From optical microscopy, the X70 steel was determined to be polygonal ferrite and either acicular ferrite or bainite. There may be other constitutents that are not resolvable without employing more advanced analytical techniques.

Table 1: Chemical compositions of the X70 pipeline steel, in mass percent.

	C	Mn	P	S	Si	Cu	Ni
Mass %	0.048	1.43	0.009	0.001	0.17	0.220	0.014
	Cr	**Mo**	**V**	**Nb**	**Ti**	**Al**	**Fe**
Mass %	0.240	0.005	0.004	0.054	0.027	0.015	Balance

Table 2: Tensile properties of the X70 pipeline steel, measured in the transverse orientation.

Yield Strength (MPa)	Ult. Tensile Strength (MPa)
509	609

METHODS

Fatigue Crack Growth Rate Measurements

Measurement of the FCGR was performed according to ASTM E647[11] for compact tension (C(T)) specimens (length W = 26.67 mm and thickness B = 3 mm) with a Crack Mouth Opening Diplacement (CMOD) gauge attached to the load line. All C(T) specimens were fatigue pre-cracked in air to obtain a sharp initial crack. The pre-crack length for all specimens was approximately 10 mm. All FCGR measurements were performed at a load ratio R = 0.5 and maximum load Pmax = 1.7 kN. A cycling frequency f = 1 Hz was used for the H2 test and a cycling frequency of f = 10 Hz was used for the air test. Research-grade (99.9995 % pure) H was used for testing. Analysis of the test gas indicated O and H2O concentrations below the detection limits of 0.5 ppm for O and 1 ppm for H2O. Figure 1 shows the FCGR for the X70 steel in air and H2.

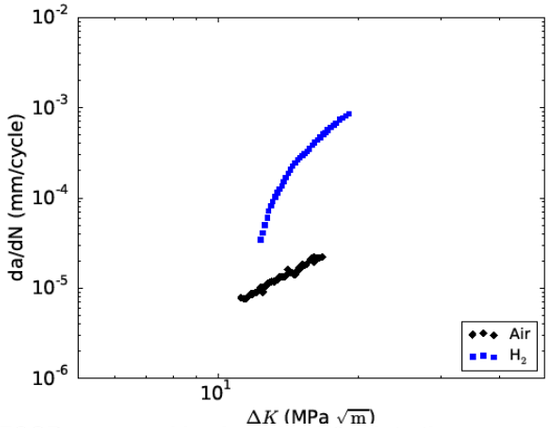

Figure 1: FCGR measured in air and in H2. Note the presence of a "knee", or a sharp increase in FCGR in the H2 data at ~ ΔK = 12 MPa m1/2.

Gas Pressure Chamber

Figure 1 shows a diagram of the test chamber utilized for this experiment. To be sufficiently transparent to neutrons and x-rays, the chamber was constructed of the aluminum alloy 6061-T6. The wall thickness of the thin portion of the chamber is 3.175 mm, which allows ≈ 95% of incident neutrons to be transmitted through the chamber.

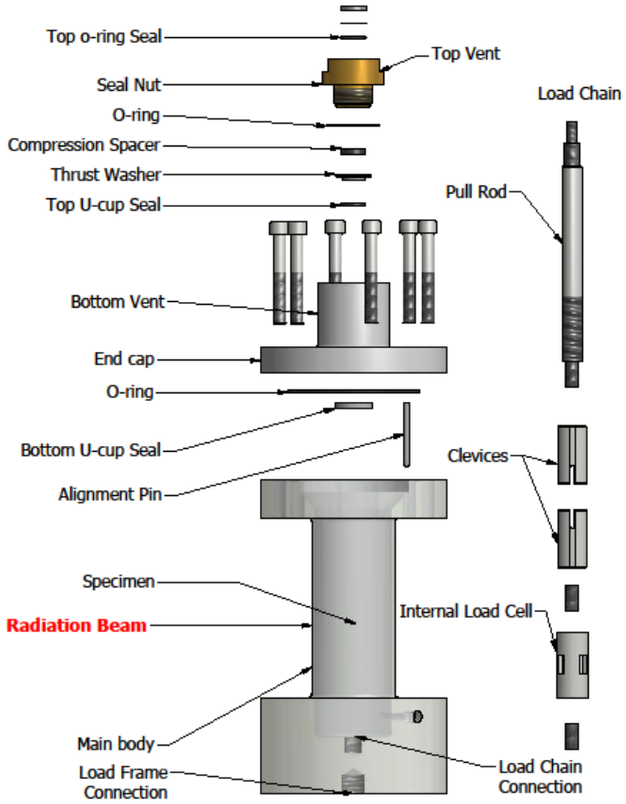

Figure 2: Schematic of the test chamber.

Strain Measurements

TBES measurements were performed at the NIST Center for Neutron Research (NCNR) NG-6 beamline[12]. This beamline uses a pyrolytic graphite double monochromator system to vary the incident neutron wavelength. A LiF pixelated detector plate was used [13]. The detector plate is 28 cm × 28 cm in area, and the pixel size is 50 μm × 50 μm. For strain measurements, a C(T) specimen with length W = 26.67 mm and thickness B = 6 mm was used. Fatigue cracks were grown with a load ratio R = 0.5, maximum load Pmax = 3.4 kN, and

a cycling frequency f =0.033 Hz. A larger Pmax was used for the strain measurements compared to the FCGR measurements because of the larger specimen thickness. The loading frequency was limited because of the constraints of a stepper motor on the load frame. Separate, identically prepared specimens were used for the in-air and in- H2 measurements. Each fatigue crack was cyclically loaded for at least N = 3000 cycles to ensure fresh crack growth in each environment. The specimens were then held at a given load for the TBES measurements. TBES employs Bragg's law[14-15]:

$$\lambda = 2\, d_{hkl} sin\theta \qquad \textbf{(1)}$$

where λ is the wavelength of incident radiation, dhkl is the lattice spacing corresponding to reflection from a particular crystallographic (hkl) plane, and θ is half of the scattering angle. For a given (hkl) reflection, the Bragg angle increases with λ until the back-scattering condition, θ = π. For larger wavelengths, λ > 2dhkl, Eqn. 1 is no longer satisfied for any θ, and therefore no scattering from that particular crystallographic plane occurs, and the transmission through the sample will increase sharply (so-called "Bragg Edge", see Fig. 3). Thus, by locating the wavelength in which a Bragg Edge occurs, the material lattice spacing can be determined. In practice, the sharp increase in transmitted intensity is smoothed by the finite wavelength resolution of the instrument. Close to the Bragg Edge, the transmitted intensity is accurately expressed as the convolution of a step function, which represents the Bragg edge, and a Gaussian function, which represents the instrument wavelength broadening. The convolution of a step and Gaussian function can be written as a complimentary error function,

$$Tr(\lambda) = A + C\ Erfc(\lambda - d_{hkl}/2\sigma) \qquad \textbf{(2)}$$

where A is a parameter related to the background intensity, C is related to the neutron scattering cross section and the thickness of the specimen, and σ is related to the full-width at half-maximum of the distribution of neutron wavelengths from instrument broadening. Figure 3 shows a sample of the transmission acquired over a 2x2 pixel area (100 μm x 100 μm), as well as the fit to Eqn. 2. Thus, a measurement of the transmission of neutrons, through a material and incident on each detector pixel, provides a route to a fast, accurate determination of the lattice spacing, d, of the material with spatial resolution governed by the pixel size. Shifts in this measured lattice spacing with respect to a reference, unstrained lattice spacing, d_0, provide a measure of the material's strain, given by

$$\varepsilon = \frac{d - d_0}{d_0} \qquad \textbf{(3)}$$

Figure 4 shows radiographs of the experimental setup using incident neutron wavelength above and below the Bragg edge.

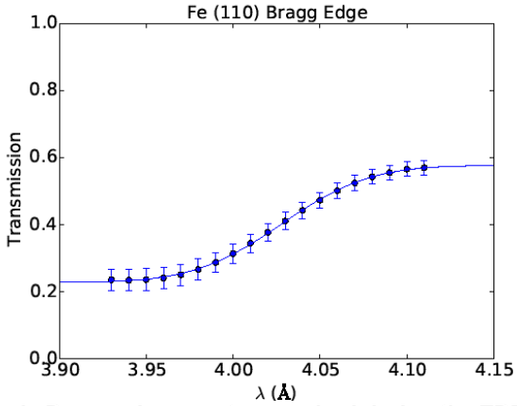

Figure 3:Sample Bragg edge spectra acquired during the TBES measurement, with fit function according Eqn 2. The transmission was averaged over a 2x2 pixel area to achieve the counting statistics indicated by the error bars.

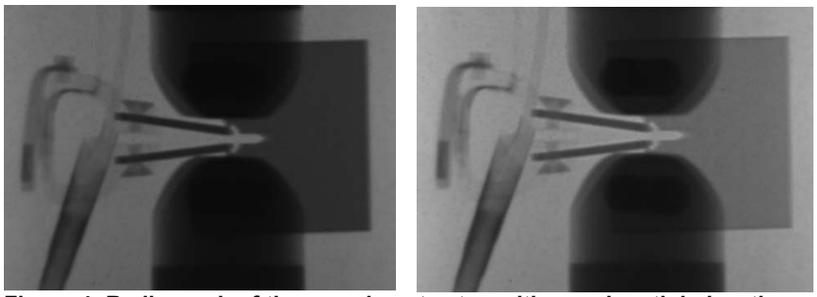

Figure 4: Radiograph of the experiment setup with wavelength below the Bragg edge (left) and above the Bragg edge (right). On the left side of each image are a clip gauge and wires associated with the load cell. In the top and bottom center the two dark areas are the two clevises, which hold the C(T) specimen during the test. The transmission through the specimen is noticeably larger for the radiograph above the Bragg edge.

RESULTS AND DISCUSSION

Contour images of the measured strain fields in air and in H2 for loading P=5.15 kN are shown in Fig. 5. The contour images show a larger compressive crack tip strain for the crack grown in H2 as compared to air. Because a tensile load is applied in the plane of the specimen, the through-thickness strain component observed via TBES is compressive. The results of this study appear to suggest that the effect of hydrogen is to enhance the crack-tip strain for a given applied load beyond that observed in air.

This result is consistent with the HEDE mechanism; as H absorbs into the material, the presence of H in the lattice decreases the Fe-Fe interaction energy, leading to larger elastic strains for a given applied load. The HEDE mechanism predicts both an intragranular decohesion, between the Fe atoms within the lattice, as well as an intergranular decohesion, between grains in the material. However, it should be emphasized that the strain measurements presented here provide only a measurement of the elastic lattice strain. Because lattice strain is measured, hydrogen-induced intergranular decohesion is not indicated in these measurements.

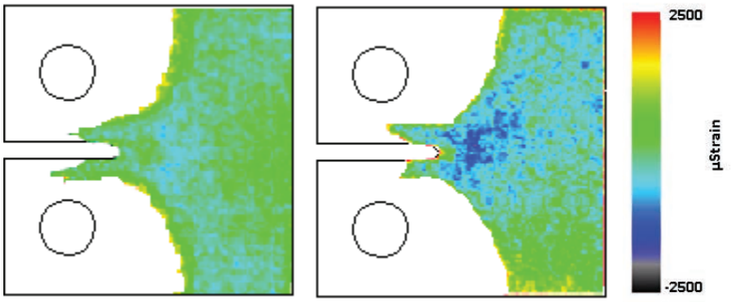

Figure 5: Measured strain fields for the cracks grown in air (left) and in H2 (right).

However, the results are consistent with an intragranular decohesion due to the presence of H2. Further, because only elastic strains are measured without any information on plasticity (ie. dislocation pileups), this measurement cannot provide evidence for, or against, the HELP mechanism. It has been argued that the increase in dislocation pileup due to the HELP mechanism likely aides in providing the large hydrogen concentrations necessary for inter- and intra-granular decohesion in the HEDE mechanism[16]. These measurements are primarily susceptible to effects of the HEDE mechanism, it is therefore likely for concurrent mechanisms to be acting.

The power in the measurements presented here is the possibility to quantify the extent of the enhanced elastic strain field ahead of the crack tip. For distances ahead of the crack tip in which the material conforms to Linear Elastic Fracture Mechanics (LEFM), the crack tip stress intensity factor, K, completely defines the stress state ahead of the crack tip. In order to achieve the enhanced elastic strain field in H2 shown here, the stress state must be characterized by a larger K than observed in air. Because ΔK is the independent variable in FCGR measurements, this quantification is crucial to understand the differences in air and H2 environment FCGR, as presented in Fig. 2. Attempts are underway to quantify these differences for a range of loads, crack lengths, and gas pressures.

CONCLUSIONS

Strain fields near fatigue crack tips that were grown in air and in H2 are presented. In H2, the magnitude and spatial extent of the strain field was enhanced

compared with the strain field in air. The results presented are consistent with a presumed intragranular HEDE mechanism contributing to the deformation. In order to fully elucidate the range over which the HEDE mechanism is exhibited, it is crucial to determine the crack-tip strain field over a larger range of applied K. In addition, the strain field must be measured as a function of H pressure, mechanical load, and crack length to provide the physics-based models with sufficient data to be fully predictive. Future measurements are planned to acquire this information, including synchrotron x-ray measurements, which will increase the spatial resolution of the measurements by a factor of $\approx$ 5. Further, the combination of elastic strain measurements with a quantification of the plasticity via the dislocation density, which can be acquired through synchroton x-ray measurements, will further elucidate the mechanisms of HA-FCG.

REFERENCES

[1] Fekete, J. R., Sowards, J. W., & Amaro, R. L. (2015). Economic impact of applying high strength steels in hydrogen gas pipelines. *International Journal of Hydrogen Energy*, *40*(33), 10547-10558.

[2] Slifka, A. J., Drexler, E. S., Nanninga, N. E., Levy, Y. S., McColskey, J. D., Amaro, R. L., & Stevenson, A. E. (2014). Fatigue crack growth of two pipeline steels in a pressurized hydrogen environment. *Corrosion Science*, *78*, 313-321.

[3] Nanninga, N. E., Levy, Y. S., Drexler, E. S., Condon, R. T., Stevenson, A. E., & Slifka, A. J. (2012). Comparison of hydrogen embrittlement in three pipeline steels in high pressure gaseous hydrogen environments. *Corrosion Science*, *59*, 1-9.

[4] Amaro, R. L., Rustagi, N., Findley, K. O., Drexler, E. S., & Slifka, A. J. (2014). Modeling the fatigue crack growth of X100 pipeline steel in gaseous hydrogen. *International Journal of Fatigue*, *59*, 262-271.

[5] Johnson, W. H. (1874). On some remarkable changes produced in iron and steel by the action of hydrogen and acids. *Proceedings of the Royal Society of London*, *23*(156-163), 168-179.

[6] Barnoush, A. (2011). Hydrogen embrittlement. *Saarland University*.

[7] Slifka, A. J., Drexler, E. S., Amaro, R., Lauria, D., Fekete, J., & Eason, K. R. (2013). Materials testing in hydrogen gas at NIST, Boulder. Retrieved August 14, 2016, from http://www.sandia.gov/matlsTechRef/advmat_presentations/Slifka_NIST.pdf

[8] Du, Y. A., Ismer, L., Rogal, J., Hickel, T., Neugebauer, J., & Drautz, R. (2011). First-principles study on the interaction of H interstitials with grain boundaries in α-and γ-Fe. *Physical Review B*, *84*(14), 144121.

[9] Moody, N. R., Thompson, A. W., Ricker, R. E., Was, G. S., & Jones, R. H. (2003). Hydrogen effects on material behavior and corrosion deformation interactions. *TMS, Warrendale, PA*.

[10] Darcis, P. P., McColskey, J. D., Lasseigne, A. N., & Siewert, T. A. (2009). Hydrogen effects on fatigue crack growth rate in high strength pipeline steel. In*Effects of Hydrogen on Materials: Proceedings of the 2008 International Hydrogen Conference, September 7-10, 2008, Jackson Lake Lodge, Grand Teton National Park, Wyoming, USA* (p. 381). ASM International.

[11] ASTM International. (2011). *Standard test method for measurement of fatigue crack growth rates*. ASTM International.

[12] Hussey, D. S., Jacobson, D. L., Arif, M., Huffman, P. R., Williams, R. E., & Cook, J. C. (2005). New neutron imaging facility at the NIST. *Nuclear Instruments and Methods in Physics Research Section A: Accelerators, Spectrometers, Detectors and Associated Equipment*, *542*(1), 9-15.

[13] Faenov, A., Matsubayashi, M., Pikuz, T., Fukuda, Y., Kando, M., Yasuda, R., ... & Kodama, R. (2015). Using LiF crystals for high-performance neutron imaging with micron-scale resolution. *High Power Laser Science and Engineering*, *3*, e27.

[14] Tremsin, A. S., McPhate, J. B., Vallerga, J. V., Siegmund, O. H. W., Feller, W. B., Bilheux, H. Z., ... & Penumadu, D. (2010). Transmission Bragg edge spectroscopy measurements at ORNL spallation neutron source. In *Journal of Physics: Conference Series* (Vol. 251, No. 1, p. 012069). IOP Publishing.

[15] Santisteban, J. R., Edwards, L., Fitzpatrick, M. E., Steuwer, A., Withers, P. J., Daymond, M. R. & Schooneveld, E. M. (2002). Strain imaging by Bragg edge neutron transmission. *Nuclear Instruments and Methods in Physics Research Section A: Accelerators, Spectrometers, Detectors and Associated Equipment*, *481*(1), 765-768.

[16] Novak, P., Yuan, R., Somerday, B. P., Sofronis, P., & Ritchie, R. O. (2010). A statistical, physical-based, micro-mechanical model of hydrogen-induced intergranular fracture in steel. *Journal of the Mechanics and Physics of Solids*, *58*(2), 206-226.

Materials Performance in Hydrogen Environments

Proceedings of the 2016

International Hydrogen Conference

September 11-14, 2016

Jackson Lake Lodge, Wyoming, USA

Edited by

B.P. Somerday

P. Sofronis

ISBN: 978-0-7918-6138-7
ASME Book Number: 861387